A Novel Crystallizable Low Band Gap Polymer for High-Efficiency Polymer Photovoltaic Cells

Xiaoli Zhao,[1,2] Hongying Lv,[1,2,3] Dalei Yang,[1,2,3] Zidong Li,[1,2,3] Zhaobin Chen,[1] Xiaoniu Yang[1,2]

[1]Polymer Composites Engineering Laboratory, Changchun Institute of Applied Chemistry, Chinese Academy of Sciences, Changchun, 130022, People's Republic of China
[2]State Key Laboratory of Polymer Physics and Chemistry, Changchun Institute of Applied Chemistry, Chinese Academy of Sciences, Changchun, 130022, People's Republic of China
[3]University of Chinese Academy of Sciences, Beijing, 100049, People's Republic of China
Correspondence to: X. N. Yang (E-mail: xnyang@ciac.ac.cn)

Received 26 June 2015; accepted 28 August 2015; published online 13 October 2015
DOI: 10.1002/pola.27916

KEYWORDS: charge transfer; conjugated polymers; crystallization; morphology; phase separation

The bulk heterojunction polymer solar cells (PSCs) have received considerable attention because of their unique advantages of light weight, flexibility and low cost production through roll-to-roll processing. During the development of PSCs, the design and synthesis of new photovoltaic materials play a critical role in realizing high power conversion efficiencies (PCEs).[1–4] For the donor polymers, narrow band gap and low highest occupied molecular orbital (HOMO) level are favorable for harvesting solar energy and improving open circuit voltage (V_{oc}), respectively.[5–9] Meanwhile, the crystalline property of polymers has an important effect on the morphology of active layer, where suitable phase separation and high crystallinity will benefit charge carrier separation, transportation and thus the device performance.[10,11] More importantly, the high crystalline has considerable contribution to the thermal stability of the bulk heterojunction morphology, which is beneficial to the practical application.[12,13] Most of highly efficient donor polymers are D-A copolymers which consist of alternant electron-rich unit (D) and electron-deficient unit (A), [14,15] and this rational design concept could effectively tune band gap, hole mobility and energy levels of copolymers, resulting in PCEs of over 10%.[16,17] However, most of the copolymers are amorphous materials and the efficiencies of devices significantly decreased at high or practical application temperature, which considerably limits their real application and commercialization.[17,18] Thus, it is useful to design and develop crystallizable low band gap D-A copolymers to get insight into the optional criteria of electron-rich unit and electron-deficient unit for such copolymers and enhance the thermal stability of the devices.

Among the electron-rich units, benzotrithiophene (BTT) has attracted many interests due to its highly planar and large electron-rich unit core, which would readily promote the effective intermolecular stacking and crystallization of polymer in the solid state.[19–21] Thus, a series of copolymers based on BTT were synthesized and applied in organic photovoltaic devices and field effect transistors.[22] However, it is necessary to further explore its potential application in design and synthesis of new semiconducting polymers with unique properties, such as enhanced crystallinity, high hole mobility, and thermal stability. Thus, a new BTT unit with modified alky chain was designed and synthesized without sacrificing its pristine Eg feature in our previous work.[23] As for the electron-deficient unit, 5,6-difluoro-4,7-di(thiophen-2-yl)benzothiadiazole (DTFFBT) is one of the famous electron-withdrawing units, which was synthesized by replacing two hydrogen atoms with two fluorine atoms in benzothiadiazole (BT) structure.[7] The introduction of the fluorine atoms not only lowers the energy levels of copolymer, but also minimizes additional steric hindrance and enhances the intra and intermolecular interactions.[24–26] Recent studies also discover that the application of fluorine atoms onto the polymer chain could suppress charge combination and thus enhance the fill factor (FF) and short circuit current (J_{sc}). Therefore, to incorporate the mentioned above advantages of DTFFBT unit and high planarity of BTT unit, a new crystallizable conjugated polymer based on BTT and DTFFBT units was designed and synthesized. This new D-A copolymer is poly[benzo[1,2-b:3,4-b':5,6-d"]trithiphene-alt-5,6-difluoro-4,7-bis(4-(2-ethylhexyl)−2-thienyl)−2,1,3-benzothiadiazole] (BTT-DTFFBT, Scheme 1). For the BTT-DTFFBT/$PC_{71}BM$ device, it is interesting that the champion PCE reached 5.61% after treated

Additional Supporting Information may be found in the online version of this article.

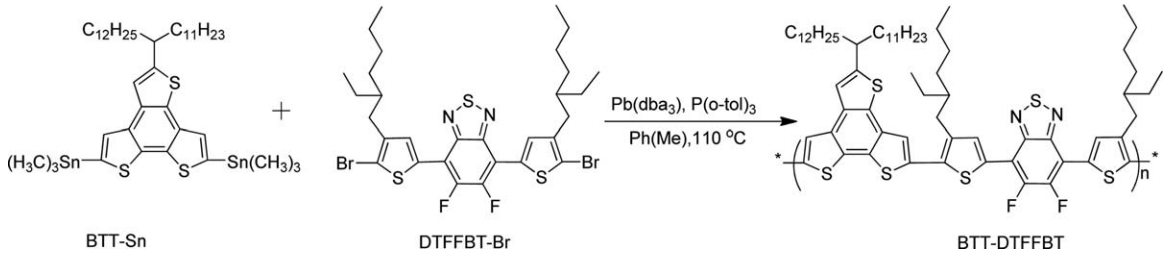

SCHEME 1 The synthetic route and structure of BTT-DTFFBT copolymer.

with CN and thermal annealed at 180 °C for 10 min. To the best our knowledge, this is the highest thermal annealing temperature to date, indicating BTT-DTFFBT shows promising potential for the high performance and thermal stability photovoltaic device.

As shown in Scheme 1, the BTT-Sn was polymerized with the DTFFBT-Br to generate the copolymer BTT-DTFFBT via Stille coupling reaction in the presence of $Pd_2(dba)_3$ as the catalyst and P(o-Tolyl)$_3$ as the ligand. The structure of BTT-DTFFBT was confirmed by H-NMR, as shown in Supporting Information Figure S1. The number average molecular weight (M_n) and polydispersity index (PDI) of BTT-DTFFBT were measured by gel permeation chromatography (GPC) in 1, 2, 4-trichlorobenzene at 150 °C with polystyrene as a standard. BTT-DTFFBT presented molecular weight with a M_n of 11,000 g mol^{-1} and a PDI of 1.22, as shown in Supporting Information Figure S2. The thermal behavior of the BTT-DTFFBT was characterized by thermogravimetric analysis (TGA), and the decomposition temperature (5% weight loss) was 420 °C for BTT-DTFFBT as shown in Supporting Information Figure S3, indicating that the BTT-DTFFBT copolymer has good thermal stability.

Figure 1 shows the UV-Vis absorption spectra of BTT-DTFFBT both in CB solution and in thin film. It was found that BTT-DTFFBT in hot solution (90 °C) displayed a main absorption peak at about 570 nm and a weak low-energy peak at around 660 nm, which could be ascribed to the intermolecular π-π interaction.[27,28] When the solution was cooled to room temperature, the main peak was obviously red-shifted from 570 to 605 nm and the π-π interaction peak became strong. Compared the BTT-DTFFBT solution at room temperature, the film showed similar absorption characteristic with an intense π-π interaction peak. The above results indicate that the polymer chains of BTT-DTFFBT could form π-π interaction even in hot solution, and this interaction could be enhanced in solution at decreased temperature and in the solid state. In addition, the optical band gap (E_{opt}) of BTT-DTFFBT was calculated to be 1.71 eV from the edge (726 nm) of absorption curve in the solid state.

Cyclic voltammetry (CV) was taken to investigate the electrochemical properties of BTT-DTFFBT as films and determine the HOMO and lowest unoccupied molecular orbital (LUMO) energy levels. The potential of Ag/Ag+ reference electrode was internally calibrated by using ferrocene/ferrocenium (Fc/Fc+) redox couple. Cyclic voltammogram of BTT-DTFFBT is shown in Supporting Information Figure S4. The HOMO and LUMO energy levels of BTT-DTFFBT were calculated from the oxidization onset (E^{ox}_{onset}) and reduction onset (E^{red}_{onset}) of CV curves by the following equations: $HOMO = -(E^{ox}_{onset} + 4.36)eV$ and $LUMO = -(E^{red}_{onset} + 4.36)$eV, respectively. Based on the calculation, the estimated HOMO and LUMO energy levels of -5.24 and -3.54 eV were obtained, respectively. From the device's point of view, the relatively low HOMO energy level is advantageous to V_{oc}, while the suitable LUMO-LUMO offset (>0.3 eV) of BTT-DTTFFDT and $PC_{71}BM$ could benefit the charge separation and transport. Since the photovoltaic performance is strongly depended on the charge carrier mobility, especially in the vertical direction of the active layer, the hole mobility (μ_h) was measured by space charge limited current (SCLC) method. The detailed device fabrication is described in the supporting information. As shown in Supporting Information Figure S5, the μ_h of BTT-DTTFFDT neat film was 6.07×10^{-5} cm^2 V^{-1} s^{-1}, while BTT-DTTFFDT/$PC_{71}BM$ composite film showed a μ_h of 2.84×10^{-4} cm^2 V^{-1} s^{-1}.

To investigate the photovoltaic performance of the new copolymer, polymer solar cells with the structure of ITO/PEDOT:PSS/BTT-DTFFBT:$PC_{71}BM$/LiF/Al were fabricated and examined under simulated AM 1.5G illumination of 100 mW cm^{-2}. The device performance was optimized by choosing

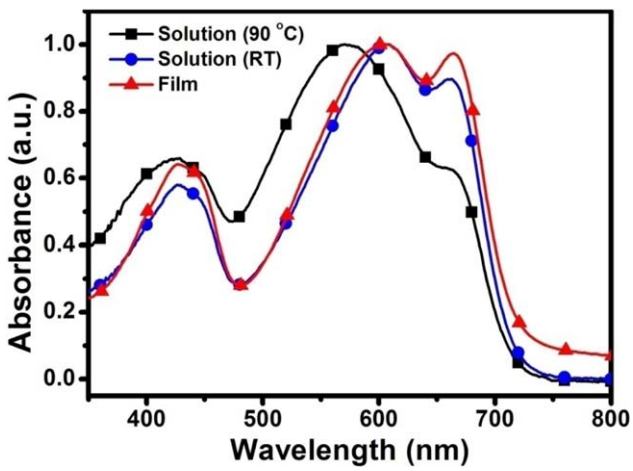

FIGURE 1 Normalized absorption spectra of BTT-DTFFBT copolymer in CB solution and in film spin-coated from CB solution. [Color figure can be viewed in the online issue, which is available at wileyonlinelibrary.com.]

different solvents, adding additive (CN), thermal annealing treatment, and inverted device structure. More details for the device optimization and characterization can be found in Supporting Information Figures S6–S7 and the corresponding photovoltaic parameters are summarized in Supporting Information Tables S2–S3.

Figure 2(a) shows the typical *J-V* curves of BTT-DTFFBT devices under different condition, and the corresponding device performance is listed in Supporting Information Table S1. For the pristine device, BTT-DTFFBT/$PC_{71}BM$ active layer was directly spin-coated from CB solution, a PCE of 2.62% was achieved. The slightly increased PCE (2.80%) was obtained for the device treated with CN additive. The relatively low *Jsc* (ca. 9.54 mA cm^{-2}) and FF (0.41) significantly limited devices performance. It is noted that the PCE of thermal annealed PSCs at 180 °C for 10 min was highly improved (4.79%) relative to that of pristine device. The device performance was further enhanced via fabricating from CB/CN (1 vol %) solution and then thermally annealing (CN+TA) at 180 °C for 10 min. For the device under this combined treatment, a J_{sc} of 11.79 mA cm^{-2}, a V_{oc} of 0.78 V and a FF of 0.61 were achieved, which resulted in a significantly enhanced PCE of 5.61%. This PCE value is higher than that of the devices under additive or thermal annealing treatment alone. Obviously, the improved device performance mainly contributed by the enhanced *Jsc* and FF. Although the additive treated device need further annealing to achieve the optimized results, the high annealing temperature indicated this polymer had a greatly potential application in fabrication thermal stable polymer solar cells. Meanwhile, Figure 2(b) shows that the combined treatment device displayed higher incident photon-to-current efficiencies (IPCE) than that of other devices in the entire absorption range of 350–700 nm, and its integrated J_{sc} from the IPCE curve was 11.75 mA cm^{-2}, which agreed well with the measured J_{sc}.

The morphology and crystallinity of the photoactive layer were investigated by TEM and XRD. As shown in Figure 3, the pristine blend film exhibited large-scale phase separation, where the size of $PC_{71}BM$ domains was in the range of 100–200 nm. These large $PC_{71}BM$ domains are greater than the diffusion length of excitons, and thus adverse to the charge separation,[29,30] resulting in low PCE (2.62%). Compared to pristine film, the large $PC_{71}BM$ domains were inhibited and the morphology became uniform for the CN-addition film. However, the device performance slightly increased to 2.80%, suggesting the crystallinity of the copolymer played a critical role in determining the device efficiency (Fig. 4). After thermal annealing for the pristine device, the phase-separation between the copolymer and PCBM domains in the active layer was more complete and BTT-DTFFBT had greater crystallinity in comparison with pristine or CN-addition film (Fig. 4); these highly ordered copolymer provided better channels for charge transport, thereby enhancing the photovoltaic performance of the devices (4.79%). It is interesting that the film under combined treatment (CN+TA) possessed suitable phase-

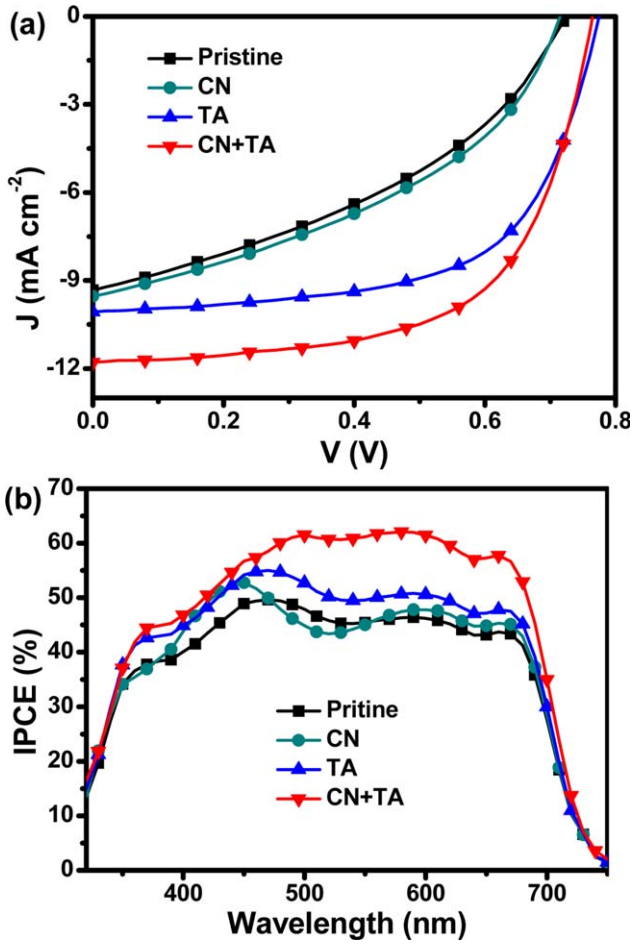

FIGURE 2 (a) *J–V* characteristics and (b) IPCE of BTT-DTFFBT/$PC_{71}BM$ devices processed from: CB solution (Pristine); CB solution containing 1 vol % CN (CN); CB solution and thermal annealed at 180 °C for 10 min (TA); CB solution containing 1 vol % CN solution and thermal annealed at 180 °C for 10 min (CN+TA). [Color figure can be viewed in the online issue, which is available at wileyonlinelibrary.com.]

separation and higher crystallinity for effective charge separation and transport, which lead to a significantly enhanced PCE of 5.61%. The results indicate that the device performance can be affected by the processing additive and thermal annealing treatment in different ways, and the combination of them gives a most effective way for the optimization of device based on BTT-DTFFBT. Meanwhile, a conventional polymer (PBDT-DTFFBT) was taken as a reference to evaluate the thermal stability of the device based on BTT-DTFFBT. These devices based on the polymers were thermally annealed at 180 °C for 60 min as accelerated durability test to characterize the device thermal stability. The typical *J-V* curves were shown in Supporting Information Figure S9 and corresponding parameters were listed in Supporting Information Table S5. It could be observed that PBDT-DTFFBT devices displayed poorer stability at high temperature and the PCE dropped significantly from 5.77 to 2.04% (PCE loss ratio: 65%), after the accelerated durability test, which was attributed to the decrease of FF and J_{sc}. In sharp contrast,

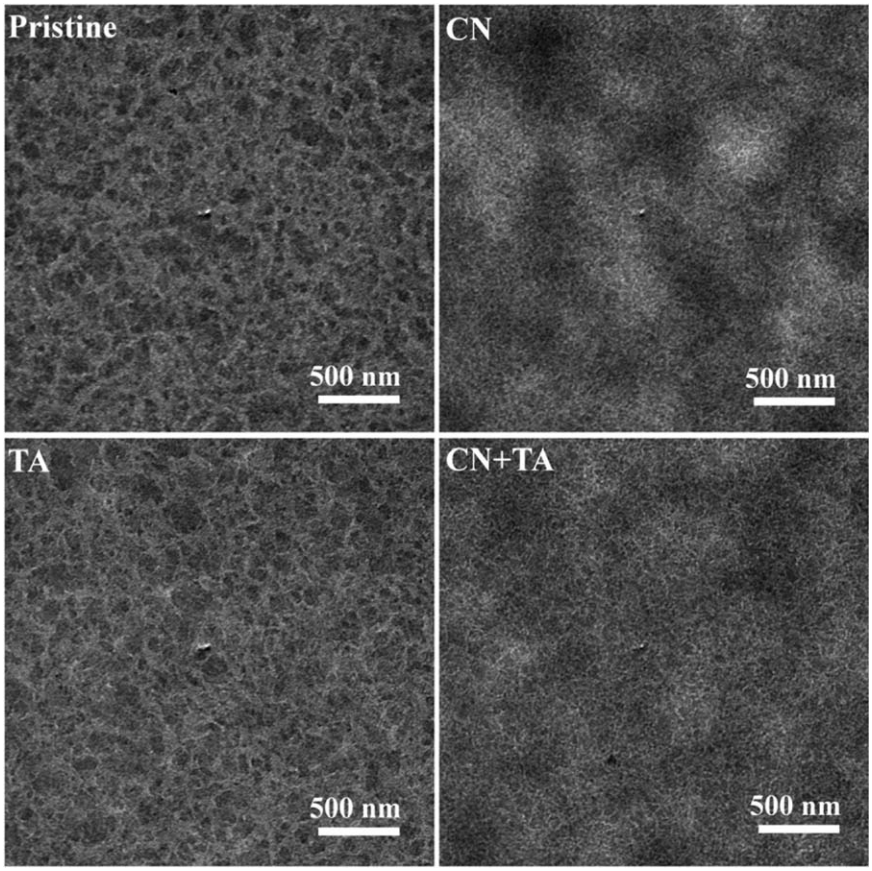

FIGURE 3 TEM of BTT-DTFFBT/$PC_{71}BM$ composite films under different condition.

BTT-DTFFBT devices exhibited the most stable performances and could preserve 84% of its original efficiency (PCE loss ratio: 16%), after the same thermal treatment process. These results demonstrated that the thermal stability of PSCs based on BTT-DTFFBT significantly enhanced as compared with PBDT-DTFFBT. Given that the molecular structures of PBDTDTFFBT and BTT-DTFFBT were similar except for the donor units, it was reasonable to speculate that the enhancement of device thermal stability arose from the introduction of the BTT unit due to its highly planar and large electron-rich unit core, which would readily promote the crystallization of polymer in the solid state and benefit the thermal stability of the device.

In conclusion, we have designed and synthesized a new crystallizable low band gap conjugated copolymer, BTT-DTFFBT, which is based on BTT and DTFFBT units. The band gap of BTT-DTFFBT was 1.70 eV with a low HOMO level of −5.24 eV. The device performance made from BTT-DTFFBT:$PC_{71}BM$ was investigated. Compared to the pristine device, PCE of CN-addition device was slightly increased from 2.62 to 2.80%, while the thermal annealing treatment improved PCE to 4.79%. Interestingly, the combination of 1 vol % CN additive and thermal annealing at 180 °C for 10 min significantly enhanced the PCE to 5.61% due to optimized phase separation and improved crystallinity. These results suggest that suitable phase-separation size and high crystallinity for the active layer and copolymer, respectively, are two key factors to determine the device performance. Importantly, the highly thermal annealing temperature is needed for the device to achieve the optimized performance, indicating that BTT-DTFFBT could be used to fabricate device with thermal

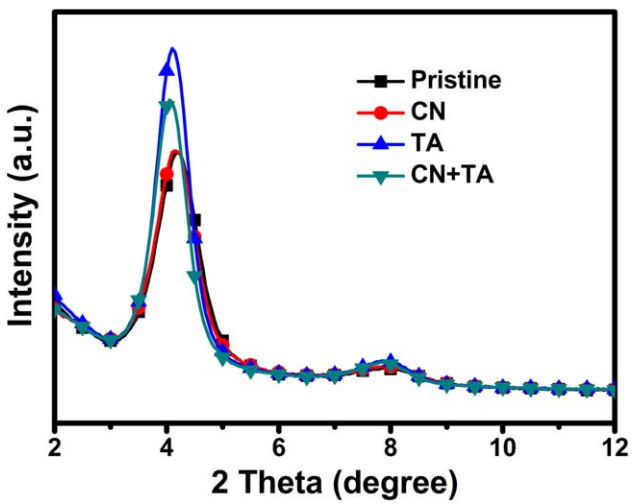

FIGURE 4 XRD profiles of BTT-DTFFBT/$PC_{71}BM$ films prepared under different condition on Si substrates. [Color figure can be viewed in the online issue, which is available at wileyonlinelibrary.com.]

stability to realize its practical application. This result also discover that BTT unit is a potential candidate for developing semiconducting polymers with high performance and thermal stability.

ACKNOWLEDGMENTS

This work was financially supported by Hi-Tech Research and Development Program (863) of China (2011AA050524), National Natural Science Foundation of China (NSFC) (Grant No. 21574132 and 21504090), and Solar Energy Initiative (Grant No.KGCX2-YW-399 + 9) of the Chinese Academy of Sciences.

REFERENCES AND NOTES

1 C. J. Brabec, S. Gowrisanker, J. J. M. Halls, D. Laird, S. J. Jia, S. P. Williams, *Adv. Mater.* **2010**, *22*, 3839–3856.

2 Y. He, Y. Li, *Phys. Chem. Chem. Phys.* **2011**, *13*, 1970–1983.

3 L. Dou, J. You, J. Yang, C. C. Chen, Y. He, S. Murase, T. Moriarty, K. Emery, G. Li, Y. Yang, *Nat. Photonics.* **2012**, *6*, 180–185.

4 S. C. Lan, P. A. Yang, M. J. Zhu, C. M. Yu, J. M. Jiang, K. H. Wei. *Polym. Chem.* **2013**, *4*, 1132–1140.

5 L. Huo, S. Zhang, X. Guo, F. Xu, Y. Li, J. Hou, *Angew. Chem. Int. Edit.* **2011**, *50*, 9697–9702.

6 Z. Fei, J. S. Kim, J. Smith, E. B. Domingo, T. D. Anthopoulos, N. Stingelin, S. E. Watkins, J. S. Kim, M. Heeney, *J. Mater. Chem.* **2011**, *21*, 16257–16263.

7 H. Zhou, L. Yang, A. C. Stuart, S. C. Price, S. Liu, W. You, *Angew. Chem. Int. Edit.* **2011**, *50*, 2995–2998.

8 A. Bhuwalka, M. D. Ewan, J. F. Mike, M. Elshobaki, B. Kobilka, S. Chaudhary, M. Jeffries-El. *J. Polym. Sci., Part a: Polym. Chem.* **2015**, *53*, 1533–1540.

9 C. L. Z. Lu, C. Du, X. Gong, Z. Bo, *Chin. J. Polym. Sci.* **2013**, *31*, 901–911.

10 L. Ye, S. Zhang, W. Ma, B. Fan, X. Guo, Y. Huang, H. Ade, J. Hou, *Adv. Mater.* **2012**, *24*, 6335–6341.

11 A. Gopal, A. Saeki, M. Ide, S. Seki, *Acs Sustainable Chem. Eng.* **2014**, *2*, 2613–2622.

12 T. L. Nguyen, H. Choi, S. J. Ko, M. A. Uddin, B. Walker, S. Yum, J. E. Jeong, M. H. Yun, T. J. Shin, S. Hwang, J. Y. Kim, H. Y. Woo, *Energy Environ. Sci.* **2014**, *7*, 3040–3051.

13 X. Liu, B. B. Y. Hsu, Y. Sun, C. K. Mai, A. J. Heeger, G. C. Bazan, *J. Am. Chem. Soc.* **2014**, *136*, 16144–16147.

14 R. Sheng, Q. Liu, M. Xiao, C. Gu, T. Hu, J. Ren, M. Sun, R. Yang, *J. Polym. Sci., Part A: Polym. Chem.* **2015**, *53*, 1558–1566.

15 O. Erlik, N. A. Unlu, G. Hizalan, S. O. Hacioglu, S. Comez, E. D. Yildiz, L. Toppare, A. Cirpan, *J. Polym. Sci., Part A: Polym. Chem.* **2015**, *53*, 1541–1547.

16 Y. Liu, C. C. Chen, Z. Hong, J. Gao, Y. Yang, H. Zhou, L. Dou, G. Li, *Sci. Rep.* **2013**, *3*,

17 J. D. Chen, C. Cui, Y. Q. Li, L. Zhou, Q. D. Ou, C. Li, Y. Li, J. X. Tang, *Adv. Mater.* **2015**, *27*, 1035–1041.

18 L. Huo, S. Zhang, X. Guo, F. Xu, Y. Li, J. Hou, *Angew. Chem. Int. Ed.* **2011**, *50*, 9697–9702.

19 S. C. Lan, P. A. Yang, M. J. Zhu, C. M. Yu, J. M. Jiang, K. H. Wei, *Polym. Chem.* **2013**, *4*, 1132–1140.

20 C. B. Nielsen, B. C. Schroeder, A. Hadipour, B. P. Rand, S. E. Watkins, I. McCulloch, *J. Mater. Chem.* **2011**, *21*, 17642–17645.

21 C. B. Nielsen, J. M. Fraser, B. C. Schroeder, J. Du, A. J. P. White, W. Zhang, I. McCulloch, *Org. Lett.* **2011**, *13*, 2414–2417.

22 C. B. Nielsen, R. S. Ashraf, N. D. Treat, B. C. Schroeder, J. E. Donaghey, A. J. P. White, N. Stingelin, I. McCulloch, *Adv. Mater.* **2015**, *27*, 948–953.

23 X. Zhao, D. Yang, H. Lv, L. Yin, X. Yang. *Polym. Chem.* **2013**, *4*, 57–60.

24 Y. Zhang, S. C. Chien, K. S. Chen, H. L. Yip, Y. Sun, J. A. Davies, F. C. Chen, A. K. Y. Jen, *Chem. Commun.* **2011**, *47*, 11026–11028.

25 S. C. Price, A. C. Stuart, L. Yang, H. Zhou, W. You, *J. Am. Chem. Soc.* **2011**, *133*, 4625–4631.

26 Y. Zhang, J. Zou, C. C. Cheuh, H. L. Yip, A. K. Y. Jen, *Macromolecules* **2012**, *45*, 5427–5435.

27 H. Y. Chen, J. H. Hou, A. E. Hayden, H. Yang, K. N. Houk, Y. Yang, *Adv. Mater.* **2010**, *22*, 371–375.

28 H. Lv, X. Zhao, Z. Li, D. Yang, Z. Wang, X. Yang, *Polym. Chem.* **2014**, *5*, 6279–6286.

29 A. Haugeneder, M. Neges, C. Kallinger, W. Spirkl, U. Lemmer, J. Feldmann, U. Scherf, E. Harth, A. Gugel, K. Mullen, *Phys. Rev. B.* **1999**, *59*, 15346–15351.

30 Y. Liang, Z. Xu, J. Xia, S. T. Tsai, Y. Wu, G. Li, C. Ray, L. Yu, *Adv. Mater.* **2010**, *22*, 135–138.